

FUTURE TREND ANALYSIS OF PRECIPITATION IN THE HAIHE RIVER BASIN BASED ON A METHOD COMBINING WAVELET AND RESCALED RANGE ANALYSES

by

Mei-Shui LI, Xiao-Hua YANG*, and Bo-Yang SUN

State Key Laboratory of Water Environment Simulation, School of Environment,
Beijing Normal University, Beijing, China

Original scientific paper
<https://doi.org/10.2298/TSCI1804571L>

Climate change has become an increasingly dominant environmental issue which has been attracting more and more attention in recent years. It is necessary to determine the cycle and trend of annual precipitation in the Haihe River Basin in the context of climate change because it is the largest river system in northern China. A combined method of rescaled range analysis and wavelet analysis is applied to identify the cycle and trend in annual precipitation based on data from 12 weather stations in the Haihe River Basin. The results of wavelet analysis show that the 12 weather stations all have the long main cycles of 35-38 years and the medium-length cycles of 22-25 years. Datong, Yuanping, Shijiazhuang, Taiyuan, Anyang, and Huimin stations have the short-length cycles of 9-11 years. The results of rescaled range analysis show that all of the Hurst exponents are greater than 0.5, which indicates that the future trend of annual precipitation will very likely follow the historical trend. Therefore, nine stations will have the downward trends, and other stations will have the upward trends in the future, according to the analysis of the historical trends by the method of wavelet analysis.

Key words: *climate change, rescaled range analysis, wavelet analysis, main cycle, future trend*

Introduction

Precipitation is regarded as the major factor affecting watershed hydrology and water resource systems, and is considered as one of the most significant indicators to reflect the effect of climate change. Therefore, precipitation has a major impact on socio-economic conditions [1-3]. Since the 20th century, as global climate change has attracted global attention, precipitation changes and its regional differences have become an important research area of global climate change [4, 5]. Meanwhile, the changes in precipitation directly affect the regional water balance and induce floods, droughts, and other natural disasters. In recent years, the drought frequency of the Haihe River Basin has often ranked first in China, with nearly nine droughts during the last ten years [6, 7]. In recent 50 years, the annual precipitation in Haihe River Basin showed a decreasing trend with a decrease of 21 mm per decade [8, 9]. Therefore, understanding the changing cycles and trends of annual precipitation in the Haihe River Basin is significantly important for preventing natural disasters and resolving conflicts between development and water resources shortage.

* Corresponding author, e-mail: xiaohuayang@bnu.edu.cn

Recently, the most methods of trend analysis are based on traditional mathematical statistics or simple smoothing method, such as Mann-Kendall (MK) method which can not reflect the multi-time scale features of hydrological sequence [10]. Wavelet analysis is a type of multi-resolution analysis in time and frequency that can effectively determine a time series signal's main frequency component, which can easily solve the problems. This has led to great advances in signal processing, image compression and encoding, tongue encoding, mode identification and non-linear science fields [11]. Wavelet analysis has become widely applied in hydrology and water resources, and has made some progress [12]. However, it is difficult to determine the future trend of a time series using wavelet analysis [13]. Therefore, the fractal theory is used in this study.

The method of fractal theory is widely used in many fields with many scientists contributing their efforts to its theory and application [14, 15]. Rescaled range (RS) analysis is a critical part of fractal theory created by Hurst [16]. It is generally used to estimate the long-range dependence of a time series. Mandelbrot has exhaustively tested the possibility of using rescaled range analysis as an empirical technique to identify hidden cycles in data sets [17, 18]. However, the work does not include a method for determining the length of such a cycle. In this paper, we combine wavelet analysis and RS analysis to find the main cycle of a meteorological data series and to predict its future trend.

Methods

Description of RS analysis

For a fractal time series, the result obtained by Mandelbrot *et al.* is [19]:

$$\frac{R(h)}{S(h)} = (ah)^H \quad (1)$$

where $R(h)/S(h)$ is the RS range, h – the time increment, a – a constant, and H – the Hurst exponent. For a given time series X_t of length N , the RS analysis is performed by the following steps [20].

Step 1. Divide $\{X_t\}$ into a contiguous subsequence of length h ($h \geq 3$) such that $Mh = N$. Each subsequence is recorded as D_m ($m = 1, 2 \dots M$) with element $sx_{k,m}$. The mean of each subsequence D_m is defined as in eq. (2):

$$\langle x \rangle_m = \frac{1}{h} \sum_{k=1}^h x_{k,m} \quad (2)$$

Step 2. Create a new time series $X_{k,m}$ representing the accumulated departures from the average for each subsequence, defined:

$$X_{k,m} = \sum_{k=1}^N (x_{k,m} - \langle x \rangle_m) \quad (N = 1, 2, \dots, h) \quad (3)$$

Step 3. Define the maximum range of each subsequence as in eq. (4):

$$R_m = \max(X_{k,m}) - \min(X_{k,m}), \quad k = 1, 2, \dots, h \quad (4)$$

Step 4. Calculate the standard deviation of each subsequence S_m :

$$S_m = \sqrt{\frac{1}{h} \sum_{k=1}^h \{x_{k,m} - \langle x \rangle_m\}^2} \quad (5)$$

Step 5. The RS range of the length h of each subsequence D_m is defined:

$$(RS)_m = \frac{R_m}{S_m} \quad (6)$$

Step 6. Repeat steps 2-6 to obtain a RS range series with rescaled range $(RS)_h$:

$$(RS)_h = \frac{1}{M} \sum_{m=1}^M (RS)_m \quad (7)$$

Step 7. We find that the RS range series of $\{X_t\}$ satisfies eq. (1) when the value of $h = 3$. Equation (8) can be obtained by taking the logarithm of eq. (1). We run a least-squares regression to find the slope H shown in eq. (8), which is the Hurst exponent:

$$\log(RS)_h = H \log a + H \log h \quad (8)$$

When $0.5 < H < 1.0$, the long-term correlation of the time series is persistent. The persistence becomes stronger as the Hurst index value approaches 1.0.

Description of wavelet analysis

(1) Wavelet function

The basic idea of wavelet analysis is to use a cluster of wavelet functions as a representation or approximation of a signal or function [21]. A wavelet function $\psi(t)$ with shock characteristics that rapidly decay to zero is one key to wavelet analysis, $\psi(t) \in L^2(R)$ is the other. This wavelet function can be defined by:

$$\int_{-\infty}^{+\infty} \psi(t) dt = 0 \quad (9)$$

Commonly used wavelet functions include the Haar, Morlet, Mexican, and Daubechis wavelets [22]. The $\psi_{a,b}(t)$ can be acquired through compressing and expanding by eq. (10):

$$\psi_{a,b}(t) = |a|^{-\frac{1}{2}} \psi \frac{t-b}{a}, \quad a, b \in R, \quad a \neq 0 \quad (10)$$

where $\psi_{a,b}(t)$ is a successive wavelet, a – the scale factor that reflects the length of the wavelet's cycle, b – the shift factor that reflects the translation in time, and R – the set of all real numbers. It is important to select appropriate wavelet functions based on the actual situation.

(2) Wavelet coefficient

For a given finite energy signal $f(t)$ with $f(t) \in L^2(R)$, the continuous wavelet transform of $f(t)$ is defined as in eq. (11) [23]:

$$W_f(a,b) = |a|^{-\frac{1}{2}} \int f(t) \bar{\psi} \frac{t-b}{a} dt \quad (11)$$

where $W_f(a, b)$ is the wavelet transform coefficient, a – the scale factor, b – the shift factor, and $\bar{\psi}[(t-b)/a]$ – the complex conjugate of $\psi[(t-b)/a]$. In practical work, the signal is often discrete and expressed as $f(k\Delta t)$ (Δt is sampling interval). In discrete form, eq. (3) becomes:

$$W_f(a, b) = |a|^{-\frac{1}{2}} \Delta t \sum_{k=1}^N \frac{k\Delta t - b}{a} f(k\Delta t) \quad (12)$$

(3) Wavelet variance

The wavelet variance can be accessed by integrating the squares of the wavelet coefficient in the b-domain [24]:

$$\text{Var}(a) = \int_{-\infty}^{+\infty} |W_f(a, b)|^2 db \quad (13)$$

Case study

The Haihe River Basin is located in northern China (112 °E-120 °E, 35 °N-43 °N). It belongs to the continental monsoon climate zone and is located in a semi-humid and semi-arid region. The basin covers an area of 318200 km², 60% of which consists of mountains in the western and northern parts, and 40% of which consists of plains in the eastern and southern parts. The average annual precipitation is 524.69 mm and the annual temperature is 10.12 °C (1956-2011). The annual runoff of the Haihe River Basin has decreased sharply by approximately 66%, from 3.24·10¹¹ m³ in the 1950s to 1.11·10¹¹ m³ at present. The water resource shortage in the Haihe River Basin has been a growing problem in recent years. To fully analyze the variations in the Haihe River Basin precipitation, twelve weather stations were selected in the Haihe River Basin, as shown in fig. 1 and tab. 1. The annual precipitation data from 1956 to 2011 for the twelve weather stations was collected from the *Integrated planning of water resources in the Haihe River Basin* [8].

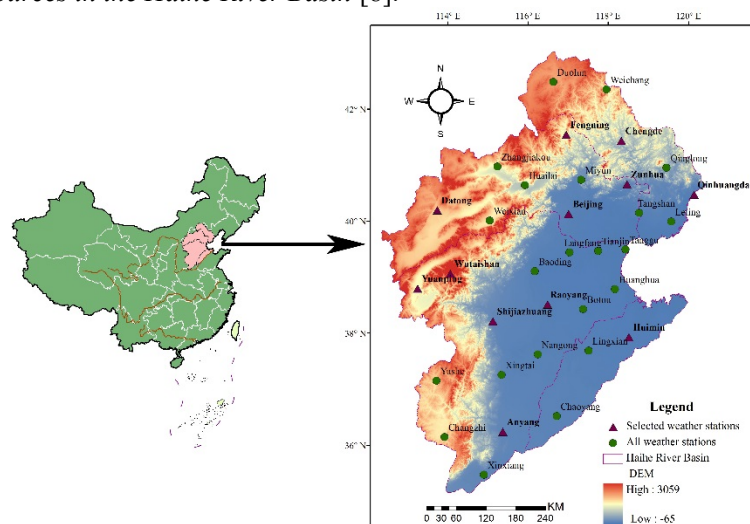


Figure 1. Weather stations of Haihe River Basin
(for color image see journal web site)

Table 1. Detail information about twelve, (a)-(l), weather stations in the Haihe River Basin

ID	Station	Time range	Location (°N,°E)
(a)	Datong	1956-2011	40.10, 113.33
(b)	Wutaishan	1956-2011	38.95, 113.52
(c)	Yuanping	1956-2011	38.73, 112.72
(d)	Shijiazhuang	1956-2011	38.03, 114.42
(e)	Taiyuan	1956-2011	37.78, 112.55
(f)	Anyang	1956-2011	36.05, 114.40
(g)	Beijing	1956-2011	39.80, 116.47
(h)	Raoyang	1956-2011	38.23,,115.73
(i)	Fengning	1956-2011	41.22, 116.63
(j)	Zunhua	1956-2011	40.20, 117.95
(k)	Huimin	1956-2011	37.48, 117.53
(l)	Qinhuangdao	1956-2011	39.85, 119.52

A continuous Morlet wavelet transform was used to calculate the wavelet coefficient, which plays an important preliminary role in deducing the cycles of annual precipitation. Figure 2 shows the real part of the wavelet coefficient, which clearly displays the changes in time and scale. Taking Shijiazhuang, fig. 2(d) and Datong, fig. 2(a) as two examples, it is obvious that the main cycles of Shijiazhuang are 10, 22, and 38 years and the main cycles of Datong are 10, 22, and 37 years because of the large square modulus gathered near these places, as shown in fig. 2.

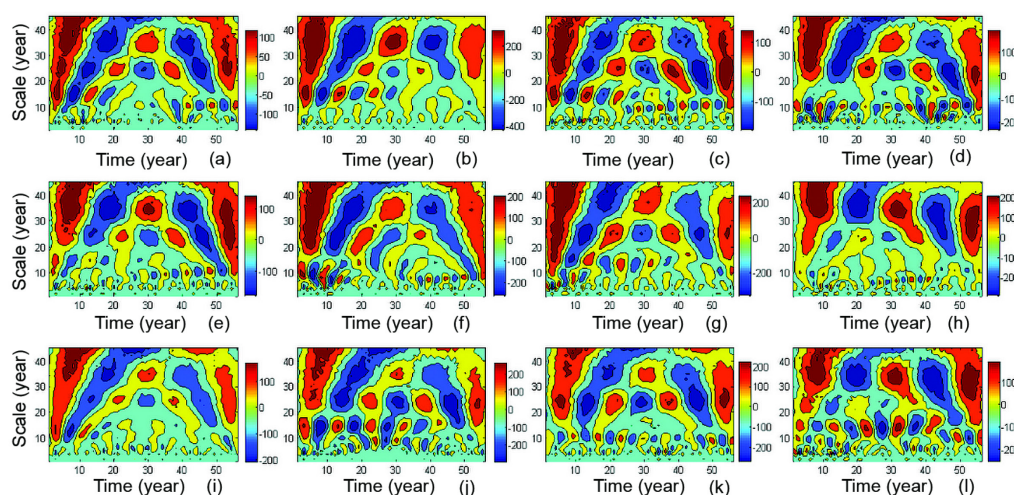


Figure 2. The real part of the wavelet coefficient by Morlet wavelet transform of annual precipitation (for color image see journal web site)

The wavelet variance was used to accurately test the cycles obtained by the wavelet coefficients. Short, medium, and long cycles are defined as having lengths of 0-15, 16-30, and 31-45 years, respectively. The wavelet variances are shown in fig. 3. Taking the Datong

weather station as an example, fig. 3(a) shows one apparent peak at 35-38 years, one insignificant peak at 22-25 years, and one insignificant peak at 9-11 years. Therefore, the long cycle of 35-38 years is considered the main cycle. Table 2 contains details of the cycles recorded at each of the 12 weather stations.

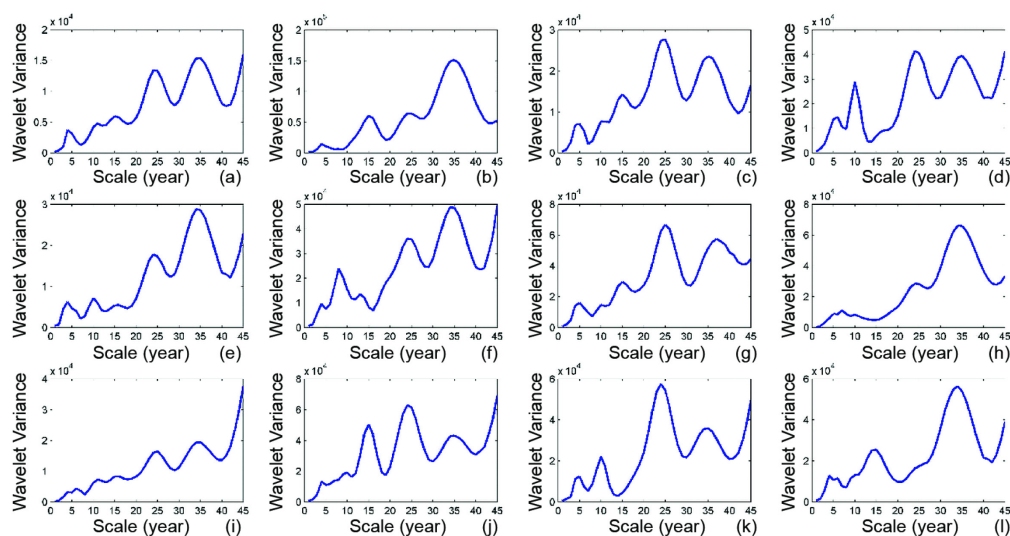


Figure 3. Wavelet variances of annual precipitation

Table 2 shows that all of the weather stations have the long cycles of 35-38 years and the medium cycle of 22-25 years. Datong, Yuanping, Shijiazhuang, Taiyuan, Anyang, and Huimin stations have the short-length cycles of 9-11 years. And other stations also have the short cycle closer to 10 years. Ren *et al.* [25] found that there was a clear cycle of 10.5 and 25 years in the past 500 years in northern China, which is consistent with the results in this paper.

Table 2. Results of cycles and RS analysis of annual precipitation time series for 12 weather stations

Station	Short cycle	Medium cycle	Long cycle	H	R^2
Datong	9-11	22-25	35-38	0.5905	0.8467
Wutaishan	—	22-25	35-38	0.7254	0.9470
Yuanping	9-11	22-25	35-38	0.6577	0.9303
Shijiazhuang	9-11	22-25	35-38	0.6206	0.9085
Taiyuan	9-11	22-25	35-38	0.7096	0.9516
Anyang	9-11	22-25	35-38	0.6769	0.9258
Beijing	10-12	22-25	35-38	0.6614	0.8996
Raoyang	8-10	22-25	35-38	0.5987	0.8804
Fengning	10-15	22-25	35-38	0.7235	0.9274
Zunhua	10-15	22-25	35-38	0.6329	0.8810
Huimin	9-11	22-25	35-38	0.5773	0.8582
Qinhuangdao	10-12	22-25	35-38	0.6220	0.8965

Considering the characteristics of time series and wavelet function, *db5* was selected to perform discrete wavelet decomposition. Daubechies *db5* contains seven parts: *s*, *a5*, *d1*, *d2*, *d3*, *d4*, and *d5*. The first part, *s*, represents the signal or raw data and the second part, *a5*, corresponds to the amplitude of the signal. The last parts: *d1*, *d2*, *d3*, *d4*, and *d5*, represent details of the signal or raw data at five different levels. In this paper, the sample size $N = 56$, and the maximum number of decomposition layers is 5, $[\log^2 56]$. The number of decomposition layers is 5 because that value will result in the smallest standard error. Comparing to MK method in tab. 3, the MK statistical test values for 12 weather stations are less than zero, which indicates the significantly downtrend in Haihe River basin. However, there are some inconsistencies here in the results obtained by the two methods. The reason may be that the length of data will cause a certain impact on the results. Wavelet analysis is more credible because the significant values by MK test are all smaller than 80% for inconsistent results between two methods.

Table 3. The future trends of annual precipitation series of 12 weather stations

Station	Wavelet analysis	Mann-Kendall		Future trend
		Trend	Confidence level [%]	
Datong	downtrend	downtrend	77.92	downtrend
Wutaishan	downtrend	downtrend	100	downtrend
Yuanping	uptrend	downtrend	62.80	uptrend
Shijiazhuang	uptrend	uptrend	45.38	uptrend
Taiyuan	downtrend	downtrend	76.83	uptrend
Anyang	uptrend	downtrend	78.35	uptrend
Beijing	downtrend	downtrend	90.43	uptrend
Raoyang	downtrend	downtrend	94.16	downtrend
Fengning	downtrend	downtrend	97.09	downtrend
Zunhua	downtrend	downtrend	98.89	downtrend
Huimin	downtrend	downtrend	72.90	downtrend
Qinhuangdao	downtrend	downtrend	78.35	downtrend

The Hurst exponent, H , can be obtained by the method of RS analysis. The future trends can be predicted based on the historical trends of annual precipitation at each weather station because all Hurst of the exponents are greater than 0.5, as shown in tab. 2. The Hurst exponents are believable because linear regression equation between $\log(R/S)_h$ and $\log h$ is strongly consistent, with all of the values of R^2 greater than 0.84. The details of the results of the RS analysis are shown in tab. 2. Table 3 displays the future trends in the annual precipitation series of the 12 weather stations. It shows that nine stations will have downward trends, and other stations will have upward trends according to the historical trends. However, the Hurst exponents of Huimin, Datong, and Raoyang stations are very close to 0.5, which may reflect some uncertainty in the future trends.

Conclusion

A combined method of RS analysis and wavelet analysis is applied to analyze the cycles and trends in annual precipitation from 1956 to 2011 based on data from 12 weather

stations in the Haihe River Basin. The results of the wavelet analysis show that the 12 weather stations all have long main cycles of 35-38 years and medium-length cycles of 22-25 years. Datong, Yuanping, Shijiazhuang, Taiyuan, Anyang, and Huimin stations have the short-length cycles of 9-11 years. The results of the RS analysis show that all of the Hurst exponents are greater than 0.5, which indicates that the future annual precipitation trend will be very likely to follow the historical trend. Nine stations will have the downward trends, and other stations will have the upward trends based on the historical trends. In conclusion, the Haihe River Basin will be very likely to suffer the effects of drought in the future.

The variability of annual precipitation are extensively influenced by climate change and human activity. Therefore, the complex impact of human activity and climate change will be the subject of a future study.

Acknowledgment

This work was supported by the National Key Research Program of China (No. 2017YFC0506603, 2016YFC0401305), the Project of the State Key Program of National Natural Science of China (No. 41530635), and the National Natural Foundation of China (No. 51679007).

References

- [1] He, J.-H., et al., The Inversion of Soil Moisture by the Thermal Infrared Data, *Thermal Science*, 17 (2013), 5, pp. 1375-1381
- [2] Fang, Q., et al., Changes of Daily Precipitation of China in Wintertime during the Last 46 Years, (in Chinese), *Scientia Geographica Sinica*, 27 (2007), 5, pp. 711-717
- [3] Yang X. H., et al., Vulnerability of Assessing Water Resources Based on the Improved Set Pair Analysis, *Thermal Science*, 18 (2014), 5, pp. 1531-1535
- [4] Liu, H., et al., Climatic Characteristics of Temperature and Precipitation in Hotan River Basin during 1954-2007 (in Chinese), *Desert and Oasis Meteorology*, 3 (2009), 4, pp. 25-29
- [5] Yang X. H., et al., Improved Gray-Encoded Evolution Algorithm Based on Chaos Cluster for Parameter Optimization of Moisture Movement, *Thermal Science*, 21 (2017), 4, pp. 1581-1585
- [6] Yan, D. H., et al., Spatial and Temporal Changes in Drought Since 1961 in Haihe River Basin (in Chinese), *Advances in Water Science*, 24 (2013), 1, pp. 34-41
- [7] Lu, L., et al., Analysis of Drought/Waterlogging Variation Tendency and Evolution Features in Haihe River Basin during 1469-2008 Years (in Chinese), *Water Resources and Power*, 4 (2011), 1, pp. 57-43
- [8] Di, C. L., et al., A Four-Stage Hybrid Model for Hydrological Time Series Forecasting, *PloS One*, 9 (2014), 8, pp. 1-10
- [9] Ding, X. Y., et al., Impacts of Climate Change on Water Resources in the Haihe River Basin and Corresponding Countermeasures (in Chinese), *Journal of Natural Resources*, 25 (2010), 4, pp. 604-613
- [10] Burn, D. H., et al., Detection of Hydrologic Trends and Variability, *Journal of Hydrology*, 255 (2002), 1, pp. 107-122
- [11] Torrence, C., et al., A Practical Guide to Wavelet Analysis, *Bulletin of the American Meteorological Society*, 79 (1998), 1, pp. 61-78
- [12] Partal, T., et al., Long-Term Trend Analysis Using Discrete Wavelet Components of Annual Precipitations Measurements in Marmara Region (Turkey), *Physics and Chemistry of the Earth, Parts A/B/C*, 31 (2006), 18, pp. 1189-1200
- [13] Kumar, P., et al., A Multicomponent Decomposition of Spatial Rainfall Fields: 2. Self-Similarity in Fluctuations, *Water Resources Research*, 29 (1993), 8, pp. 2533-2544
- [14] Basingthwaighte, J. B., et al., Evaluating Rescaled Range Analysis for Time Series, *Annals of biomedical engineering*, 22 (1994), 4, pp. 432-444
- [15] Li, Yu-Qi, et al., Spatial and Temporal Distribution of Moisture Migration in Bio-Retention Systems, *Thermal Science*, 18 (2014), 5, pp. 1557-1562
- [16] Hurst, H. E., Long Term Storage Capacity of Reservoirs, *Trans American Society of Civil Engineers*, 116 (1951), 12, pp. 776-808

- [17] Yan, A. L., et al., Study on Complex Property of the Runoff Time Series Based on R/S Method, *Journal of Applied Sciences*, 25 (2007), 2, pp. 214-217
- [18] Yu, Y. S., et al., Analysis of Future Trend Characteristics of Hydrological Time Series Based on R/S and Mann-Kendall Methods, *Journal of Water Resources and Water Engineering*, 3 (2008), pp. 011
- [19] Mandelbrot, B. B., et al., Fractional Brownian Motions, Fractional Noises and Applications, *SIAM Review*, 10 (1968), 4, pp. 422-437
- [20] Qu, G. Z., et al., Analysis of Water Resources Variation of Yellow River and Main River in the Loess Plateau with R/S Method, *Journal of Desert Research*, 30 (2010), 2, pp. 467-470
- [21] Wang, X. J., et al., The Evolvement Characteristics and Wavelet Analysis of Spring Precipitation of Last 40 Years in East Qinghai, *Agricultural Research in the Arid Areas*, 24 (2006), pp. 21-25
- [22] Elsanabary, M. H., et al., Wavelet Analysis of Seasonal Rainfall Variability of the Upper Blue Nile Basin, its Teleconnection to Global Sea Surface Temperature, and its Forecasting by an Artificial Neural Network, *Monthly Weather Review*, 142 (2014), 4, pp. 1771-1791
- [23] Zhuang, X., et al., Wavelet Characteristics of Climate Change in Beijing Since the 19th Century (in Chinese), *Acta Meteorologica Sinica*, 58 (2000), 3, pp. 362-369
- [24] Wang, Z. L., et al., Runoff Variation and its Impacting Factors in the Dongjiang River Basin During 1956-2005 (in Chinese), *Journal of Natural Resources*, 25 (2010), 8, pp. 1365-1374
- [25] Ren, G. Y., et al., Multi-Time-Scale Climatic Variations over Eastern China and Implications for the South-North Water Diversion Project, *Journal of Hydrometeorology*, 12 (2011), 4, pp. 600-617